



Magnetic resonance imaging reveals distinct bone marrow patterns in indolent and advanced systemic mastocytosis

Philipp Riffel¹ · Mohamad Jawhar² · Kristina Gawlik² · Juliana Schwaab² · Henrik J. Michaely³ · Georgia Metzgeroth² · Wolf-Karsten Hofmann² · Stefan O. Schoenberg¹ · Andreas Reiter²

Received: 12 March 2019 / Accepted: 19 October 2019 / Published online: 5 November 2019
© Springer-Verlag GmbH Germany, part of Springer Nature 2019

Abstract

Systemic mastocytosis (SM) is broadly subcategorized according to mast cell (MC) burden and organ involvement into indolent (ISM), smoldering (SSM), and advanced SM (AdvSM). However, the pattern and extent of bone involvement remains controversial. In this institutional review board (IRB)-approved study, 115 patients with different forms of SM (ISM ($n = 37$, 32%), SSM ($n = 9$, 8%), and AdvSM ($n = 69$, 60%)) underwent a whole-body magnetic resonance imaging including sagittal and coronal T1 and turbo inversion recovery magnitude (TIRM) sequences of the spine. The evaluation included the pattern and extent of pathologic bone marrow (BM) signals in the spine and extremities, osteolytic lesions, and vertebral fractures. A pathologic BM pattern was observed in 4/37 (11%), 8/9 (89%), and 66/69 (96%); affection of the appendicular skeleton in 3/37 (8%), 8/9 (89%), and 67/69 (97%); and vertebral fractures in 7/37 (19%), 0/9, and 13/69 (19%) patients with ISM, SSM, and AdvSM, respectively. In AdvSM, pathologic BM pattern included activated (62%), diffuse sclerotic (25%), and small-spotted BM (9%), respectively. Only activated/sclerotic BM was associated with significantly higher MC burden, organ damage, and inferior median survival (2.9 years, $p = 0.04$). Vertebral fractures resembled classical multi-segmental osteoporotic fractures in ISM but not in AdvSM in which they were only found in activated/sclerotic BM. Only one patient with AdvSM had a focal osteolytic lesion in the femur. Activated/sclerotic BM changes of the spine and affection of the appendicular skeleton are indicative for SSM or AdvSM. Osteolytic lesions, which are very rare, and osteoporotic fractures are ineligible for the diagnosis of AdvSM.

Keywords Systemic mastocytosis · Magnetic resonance imaging · Bone marrow · Osteolytic lesions · Osteoporosis

Introduction

Systemic mastocytosis (SM) is a rare myeloid neoplasm characterized by the accumulation of neoplastic mast cells (MCs) in bone marrow (BM) and various organ systems, e.g., skin,

skeleton, and visceral organs [1–3]. SM is broadly subcategorized into indolent SM (ISM), smoldering SM (SSM), and advanced SM (AdvSM). AdvSM includes the subtypes SM with associated hematologic neoplasm (SM-AHN), aggressive SM (ASM), and mast cell leukemia (MCL) [4]. ISM patients usually present with a low MC burden (BM MC infiltration, serum tryptase, *KIT* D816V allele burden) and little or no evidence of organomegaly (normal life expectancy); SSM is associated with a high MC burden, organomegaly but no organ damage (prognosis less favorable), while AdvSM is associated with a high disease burden, related organ damage and poor prognosis (median survival 2–4 years) [5–12].

The involvement of the skeleton in terms of osteopenia, osteoporosis, vertebral fractures, and osteolytic lesions has an important impact on the patients' quality of life and requires a careful diagnostic workup as basis for adequate treatment decisions. However, little is known about the specific pattern and extent of bone involvement within the various subtypes of SM. Studies with large numbers of patients are

Philipp Riffel and Mohamad Jawhar contributed equally to this work.

Electronic supplementary material The online version of this article (<https://doi.org/10.1007/s00277-019-03826-4>) contains supplementary material, which is available to authorized users.

✉ Mohamad Jawhar
Mohamad.jawhar@medma.uni-heidelberg.de

¹ Institute of Clinical Radiology and Nuclear Medicine, University Hospital Mannheim, Heidelberg University, Mannheim, Germany

² Department of Hematology and Oncology, University Hospital Mannheim, Heidelberg University, Mannheim, Germany

³ MVZ Radiologie Karlsruhe, Karlsruhe, Germany

rare and currently available data are predominantly derived from case reports and studies with small sample sizes [3, 13–21].

We therefore sought to evaluate the pathologic bone marrow (BM) pattern in the spine and extremities, osteolytic lesions and pathologic vertebral fractures in 115 SM patients with ISM, SSM, and AdvSM through whole-body magnetic resonance imaging (WB-MRI) and to correlate the data with clinical characteristics and survival.

Methods

Patients

This institutional review board (IRB)-approved retrospective study included 115 consecutive patients (male, $n = 67$ [58%], median age 62 years, range 22–82). SM was diagnosed in the presence of one major (dense clusters of > 15 MCs in BM or other tissues) and one of four minor criteria (spindle-shaped MCs, positivity of MC for CD25 or CD2, positivity for *KIT* D816V point mutation, serum tryptase levels > 20 $\mu\text{g/L}$) or the presence of three minor criteria. [4] Diagnosis of SSM was established through the presence of at least two of three B-findings: (a) MC infiltration > 30% and serum tryptase level > 200 ng/mL; (b) signs of dysplasia or myeloproliferation in non-mast cell lineage compartments of the BM, but no AHN; and (c) hepatomegaly without impairment of liver function and/or splenomegaly and/or lymphadenopathy [22].

Diagnosis of ASM was based on the presence of one or more C-findings: (a) one or more cytopenias (neutropenia < $1 \times 10^9/\text{L}$, anemia < 10 g/dL, or thrombocytopenia < $100 \times 10^9/\text{L}$), (b) hepatomegaly with elevated liver enzymes and impaired liver function [e.g., portal hypertension, ascites, hypalbuminemia], (c) hypersplenism with thrombocytopenia, (d) gastrointestinal involvement with malabsorption leading to significant weight loss and hypalbuminemia, and (e) presence of large osteolytic lesions and/or pathological fractures [2, 22]. The concurrent presence of SM and an associated non-mast cell hematological neoplasm defines SM-AHN. Diagnosis of MCL was based on the presence of $\geq 20\%$ MCs in BM smears.

MR imaging

All measurements were performed on a 32-channel 1.5 T WB-MRI scanner (Siemens MAGNETOM Avanto, Siemens Healthcare Sector, Erlangen, Germany) with a gradient strength of 45 mT/m and slew rate of 200 mT/m/ms. This MR scanner is equipped with the total imaging matrix that allows for complete coil coverage of the entire patient for signal reception with high quality. After the localizer four steps of coronal T1-weighted (w) and turbo inversion recovery magnitude (TIRM)-sequences were

acquired and composed to yield whole-body depictions of the patients. The first step comprised the head and thorax, the second abdomen and pelvis, the third thighs, and the last calves of the patients. Subsequently, sagittal spine images with T1w and TIRM sequences were acquired in two steps: the first, extending from the skull base to the middle of the thoracic spine and the second, from there to the end of the coccygeal bone. A detailed overview of the sequence parameters is given in supplementary material 1.

Image analysis

All patient data were reviewed by an attending radiologist with 8 years of experience in body MRI on a commercially available MacPro workstation (Apple, Cupertino, CA, USA) running OsiriX DICOM Viewer 64-bit Version 5.5.2 (OsiriX Foundation, Geneva, Switzerland) without knowledge of the clinical findings or classification. The radiologist assessed the BM of the spine on the sagittal T1w and TIRM images. The following basic patterns were differentiated:

1. Normal BM (T1 (slightly) hyperintense, TIRM slightly hyperintense, or slightly hypointense)
2. Activated BM (diffusely T1 hypointense, TIRM hyperintense)
3. Diffuse sclerotic BM (diffusely T1 hypointense, TIRM hypointense)
4. Small-spotted sclerotic BM (small-spotted T1 hypointense, TIRM hypointense)
5. Osteolytic lesions (sharply demarcated T1 hypointense, TIRM hyperintense lesion)

An overview of the different pathologic BM patterns is shown in Fig. 1. The radiologist also assessed the presence of vertebral fractures and the affection of the appendicular skeleton (no affection, diffuse affection, small-spotted affection, focal osteolytic lesions).

Statistical analysis

All statistical analyses considered clinical and laboratory parameters obtained at the time of diagnosis or first referral to our center that, in most instances, coincided with the time of BM biopsy and study sample collection. The Mann-Whitney U test was used to compare continuous variables and medians of distributions. For categorical variables, Fisher's exact test was used. OS analysis was considered from the date of diagnosis to date of death or last contact. OS probabilities were estimated with the Kaplan-Meier method and compared by the log-rank test in univariate analysis. For the estimation of hazard ratios (HRs) and multivariate analysis, the Cox proportional hazard regression model was used. p values of < 0.05 (two-sided) were considered as significant. There was no adjustment for multiple testing as all analyses were

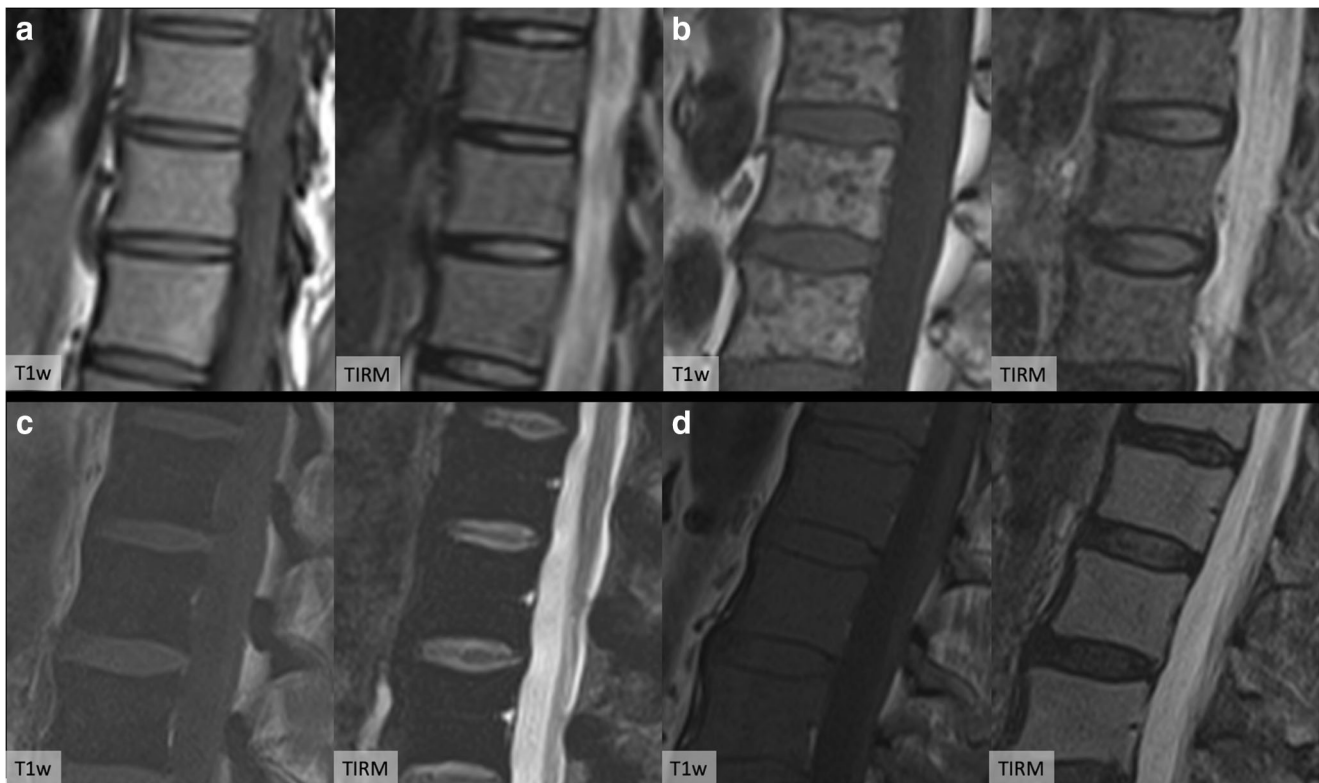


Fig. 1 Sagittal view of typical spine bone marrow (BM) patterns encountered in patients with indolent systemic mastocytosis (ISM, **a**, normal BM) and advanced SM (AdvSM) with small-spotted (**b**) sclerotic (**c**) and activated (**d**) BM, respectively

explorative. SPSS version 22 (IBM Corporation, Armonk, NY, USA) was used for statistical analysis.

Results

Patient characteristics

ISM was diagnosed in 37/115 (32%), SSM in 9/115 (8%), and AdvSM in 69/115 (60%) patients. The *KIT* D816V mutation was identified in 111/115 (97%) patients; one patient each was positive for *KIT* D816Y and *KIT* F522C mutation, respectively.

Relevant SM-associated disease characteristics of AdvSM patients are shown in Table 1. In AdvSM, the median age was 70 years (range 28–82). The median percentage of MCs in BM trephine biopsies was 30% (range 5–100). Blood parameters analyzed in this study included hemoglobin (median 10.9 g/dL, range 6.5–15.8; <10 g/dL in 38% of patients) and platelets (median $114 \times 10^9/L$, range 12–549; < $100 \times 10^9/L$ in 43% of patients). Median serum tryptase level (normal value <11.4 $\mu\text{g/L}$) was 186 $\mu\text{g/L}$ (range 13–1675; >200 $\mu\text{g/L}$ in 45% of patients). Signs of non-hematologic organ damage included elevated alkaline phosphatase (AP, median 226 U/L; range 54–1736; >150 U/L in 68% of patients), splenomegaly (86%), and ascites (43%) (Table 1). The median

KIT D816V allele burden in peripheral blood was 30% (range 0.2–67). At least one mutation in the *SRSF2*, *ASXL1*, and *RUNX1* (S/A/R) gene panel (high-molecular risk profile) was identified in 64% of AdvSM patients. The median observation time of AdvSM patients was 34 months (range 1–283); 43/69 (62%) patients have died in the observation period. The median OS was 3.8 years (95% confidence interval [CI] 2.5–5.0).

MRI-based bone marrow pattern of the spine and the appendicular skeleton

Overall, 78/115 (68%) patients revealed a pathological BM pattern of the spine. Pathologic BM signal of the spine included activated BM in 41% (47/115), diffuse sclerotic BM in 19% (19/115), and small-spotted BM in 10% (12/115). Twelve of 46 (26%) ISM/SSM patients and 66/69 (96%) AdvSM patients revealed a pathologic BM signal, respectively ($p < 0.0001$). Within the ISM/SSM patients, 4/37 (11%) of ISM patients (small-spotted BM, $n = 3$; activated BM, $n = 1$) and 8/9 (89%) of SSM patients (small-spotted, $n = 3$; activated BM, $n = 3$; diffuse sclerotic, $n = 2$) revealed a pathologic BM signal ($p < 0.0001$).

Within the AdvSM cohort, a pathologic BM signal included small-spotted BM $n = 6$ (9%), activated BM in $n = 43$ (62%), and diffuse sclerotic BM in $n = 17$ (25%) (Fig. 1).

Table 1 Clinical parameters of 69 patients with advanced systemic mastocytosis (AdvSM) with distinct bone marrow (BM) pattern in whole-body magnetic resonance imaging (WB-MRI)

BM pattern	All (<i>n</i> = 69)	Normal (<i>n</i> = 3)	Small-spotted (<i>n</i> = 6)	Activated (<i>n</i> = 43)	Sclerotic (<i>n</i> = 17)	<i>p</i> value* normal/small-spotted vs activated/sclerotic
Age, in years, median (range)	70 (28–82)	69 (30–71)	73 (55–80)	70 (28–82)	71 (49–80)	n.s.
WHO subtypes (AdvSM)						
ASM, <i>n</i> (%)	6 (9)	2 (67)	0	3 (7)	1 (6)	n.s.
MCL, <i>n</i> (%)	16 (23)	0	1 (17)	9 (21)	6 (35)	n.s.
SM-AHN, <i>n</i> (%)	47 (68)	1 (33)	5 (83)	31 (72)	10 (59)	n.s.
B-findings						
MC infiltration in BM, %; median (range); > 30%, <i>n</i> (%)	30 (5–100); 27 (39)	15 (5–20); 0 (0)	20 (10–60); 1 (20)	30 (5–100); 18 (42)	30 (20–90); 8 (47)	0.039; n.s.
Serum tryptase (µg/L); median (range); > 200, <i>n</i> (%)	186 (13–1675); 31 (45)	61 (13–160); 0 (0)	111 (18–1030); 1 (17)	188 (24–1250); 20 (47)	225 (23–1675); 9 (53)	n.s.; 0.033
Alkaline phosphatase, U/L; median (range); > 150, <i>n</i> (%)	226 (54–1736); 47 (68)	64 (61–244); 1 (33)	88 (54–283); 2 (33)	229 (55–1736); 32 (74)	259 (76–552); 12 (71)	0.003; 0.021
Spleen volume, mL; median (range); ≥ 450 mL, <i>n</i> (%)	831 (194–3193); 54 (86)	833 (402–1264); 2 (100)	628 (347–1055); 4 (88)	828 (214–2520); 35 (88)	886 (194–3193); 14 (88)	n.s.; n.s.
Liver volume, mL; median (range); ≥ 2400, <i>n</i> (%)	2286 (779–4201); 29 (46)	1825 (1783–1867); 0 (0)	1774 (779–2668); 0 (20)	2454 (1168–4201); 21 (51)	2296 (1604–3322); 7 (47)	0.022; n.s.
Lymphadenopathy, <i>n</i> (%)	45 (65)	1 (33)	3 (50)	30 (70)	11 (65)	n.s.
C-findings						
Hemoglobin, g/dL; median (range); < 10 g/dL, <i>n</i> (%)	10.9 (6.5–15.8); 26 (38)	14.2 (10.8–15.8); 0 (0)	9.3 (6.5–14.8); 4 (67)	11 (7.5–14.5); 13 (30)	9.6 (6.8–15.2); 9 (53)	n.s.; n.s.
Platelets/mL; median (range); < 100/mL, <i>n</i> (%)	114 (12–549); 30 (43)	275 (85–549); 1 (33)	144 (12–374); 3 (50)	127 (12–481); 17 (40)	91 (18–501); 9 (53)	n.s.; n.s.
Ascites, <i>n</i> (%)	30 (43)	1 (33)	1 (17)	22 (51)	6 (35)	n.s.
Albumin, g/L; %; median (range); < 35, <i>n</i> (%)	37 (19–48); 23 (38)	41 (41–43); 0 (0)	41 (26–46); 1 (17)	37 (19–48); 9 (26)	35 (22–44); 9 (56)	0.003; n.s.
Other relevant findings						
<i>KIT</i> D816V allele burden (PB), %; median (range); > 30, <i>n</i> (%)	30 (0–67); 30 (46)	7 (0.2–10); 0 (0)	4 (1–41); 1 (17)	30 (0–67); 19 (46)	37 (0–54); 8 (47)	0.001; 0.028
≥ 1 mutation in the S/A/R gen panel, <i>n</i> (%)	42 (64)	0 (0)	2 (33)	28 (67)	12 (71)	0.042

**p* values refer to Mann-Whitney *U* test or Fisher's exact test comparing patients with normal/small-spotted BM and activated/sclerotic BM
 MC, mast cell; PB, peripheral blood; S/A/R, *SRSF2*, *ASXL1*, *RUNX1*

An overview of the distribution of BM changes in the different subgroups is shown in Fig. 2.

Three of 37 (8%) ISM patients showed affection of the appendicular skeleton with a small-spotted pattern. Eight of 9 (89%) of SSM patients showed affection (small-spotted, $n = 3$; diffuse involvement, $n = 5$) of the appendicular skeleton. Almost all AdvSM patients ($n = 67$, 95%) showed affection of the appendicular skeleton (small-spotted, $n = 5$; diffuse involvement, $n = 61$) (Fig. 3).

Distinct bone marrow pattern—correlation with clinical characteristics and outcome

The median MC infiltration in BM histology, frequency of serum tryptase $> 200 \mu\text{g/L}$, median *KIT* D816V allele burden, frequency of *KIT* D816V allele burden $> 30\%$, the median liver volume, median AP, and frequency of AP $> 150 \text{ U/L}$ were all significantly higher in AdvSM patients with activated/sclerotic BM compared to normal/small-spotted BM ($p < 0.05$, Table 1). Interestingly, the number of patients with at least one mutation in the *S/A/R* gene panel was higher in the activated/sclerotic BM cohort compared to normal/small-spotted BM cohort. The median OS of the activated/sclerotic BM cohort was 2.9 years (95% CI 1.3–4.6) and was not reached for the normal/small-spotted BM cohort ($p = 0.04$, Fig. 4).

Pathological fracture of the spine and appendicular skeleton

Fractures were present in 7/37 (19%) ISM patients, in 0/9 (0%) SSM patients, and in 13/69 (19%) of AdvSM patients, respectively. All fractures were found in the spine. Interestingly, 7/7 (100%) ISM patients with vertebral fractures showed a normal BM pattern which—from a radiologic point of view—primarily resembled classical multi-segmental osteoporotic fractures (Fig. 5). In contrast, 12/13 (92%) AdvSM

patients with vertebral fractures showed pathological BM changes, including activated BM ($n = 8$, 67%) or sclerotic BM ($n = 4$, 33%), respectively (Fig. 4). No patient with ISM/SSM or AdvSM had a pathological fracture in the appendicular skeleton.

Osteolytic lesions

Osteolytic lesions were not seen in ISM/SSM. One of 69 (1.4%) AdvSM patients had a focal osteolytic lesion (Fig. 6).

Discussion

A distinct clinical feature of SM and its various subtypes is the highly variable pattern of bone involvement [23–28]. Data from X-ray and bone density studies suggested that the prevalence of detectable bone involvement in SM can be as high as 50% [29]. A recent CT study in a small series of patients described three distinct types of bone involvement including diffuse marbled sclerotic, diffuse mottled osteopenic, and focal sclerotic bone lesions. However, no statistically significant differences were reported upon the relative frequency of osseous abnormalities in ISM and AdvSM [16]. By now, two smaller series investigated the bone patterns by using MRI only, but neither differentiated between the various SM subtypes [18, 19, 30]. They rather presented different imaging patterns that might be found in patients with SM in general.

In our large cohort of patients with ISM, SSM, and AdvSM, the vast majority of ISM patients did not present with a pathological BM pattern of the spine and a diffuse sclerotic BM was not observed in any patient. Two of the four ISM patients with a pathologic BM pattern in the spine as well as all three patients with affection of the appendicular skeleton showed markedly elevated serum tryptase levels (range 77–179 $\mu\text{g/L}$) compared to the

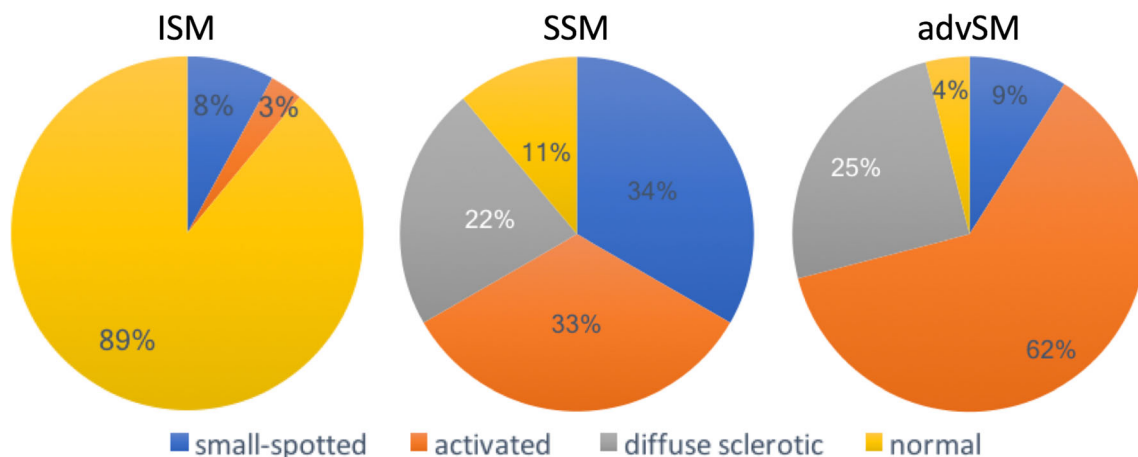
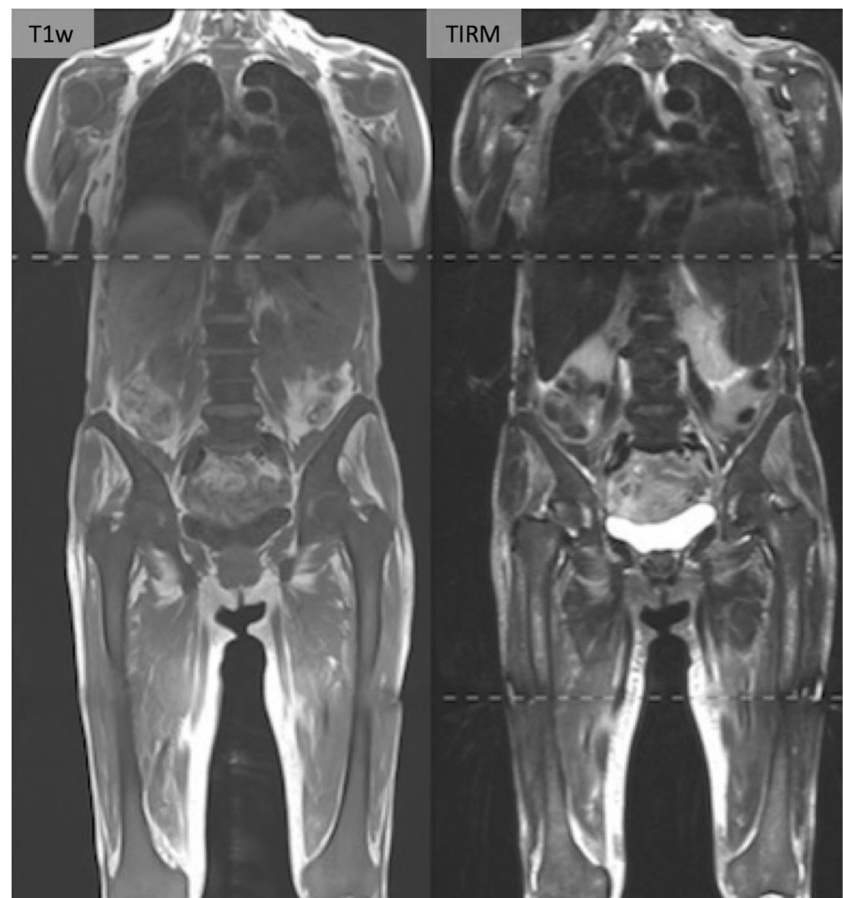


Fig. 2 Distribution of bone marrow (BM) changes in patients with indolent systemic mastocytosis (ISM), smoldering SM (SSM), and advanced SM (AdvSM)

Fig. 3 Advanced systemic mastocytosis (AdvSM) with diffuse sclerosis of the spine (dark in T1w and TIRM) as well as diffuse affection of the appendicular skeleton in a 67-year-old female patient: the entire pelvis and the depicted parts of the femurs are involved



median tryptase level of all ISM patients (36 $\mu\text{g/L}$) indicating a high MC burden. In contrast, all but one patient with SSM had a pathologic BM pattern of the spine. However, the single patient without a pathologic BM pattern revealed an involvement of the appendicular skeleton, both features which are usually indicative for AdvSM.

One of the non-quantifiable C-findings for diagnosis of AdvSM is the presence of pathological fractures. However, our data show that this criterion might be not suitable for differentiating AdvSM and ISM. In our study, vertebral fractures were

identified in 19% of patients with ISM. All patients showed a normal BM pattern which—from a radiologic point of view—primarily resembled classical multi-segmental osteoporotic fractures. This is consistent with previous studies, showing osteoporosis in 20% of patients with ISM [31] and supports the hypothesis of diffuse decrease of bone density in ISM due to mediator-release like heparin [32], histamine, or cytokines [1, 33–35]. Similar to previous reports [36], vertebral fractures were also observed in 19% of AdvSM patients. Because the vast majority of AdvSM patients revealed a pathologic BM pattern including activated and sclerotic BM, the mechanism of action may primarily be caused by the extent of MC infiltration rather than by mediator-release associated osteoporosis as observed in ISM.

According to the WHO classification, osteolytic lesions represent another important C-finding for the diagnosis of AdvSM. Consistent with previous cross-sectional studies [16] and an X-ray study reporting osteolytic lesions to be very rare in SM [29], we could not identify, however, osteolytic lesions of the spine in any patient. One patient presented with a focal osteolytic lesion of the femur. The most likely reason for the high prevalence of osteolytic lesions in previous, predominantly X-ray studies may be that normal, non-sclerotic BM surrounded by inhomogeneous and patchy sclerosis was misinterpreted as an osteolytic lesion (supplementary material 2).

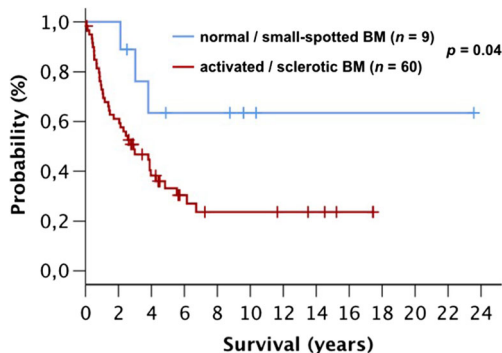


Fig. 4 Kaplan-Meier estimates of overall survival comparing advanced systemic mastocytosis (AdvSM) patients with normal/small-spotted bone marrow (BM) and AdvSM patients with activated/sclerotic BM

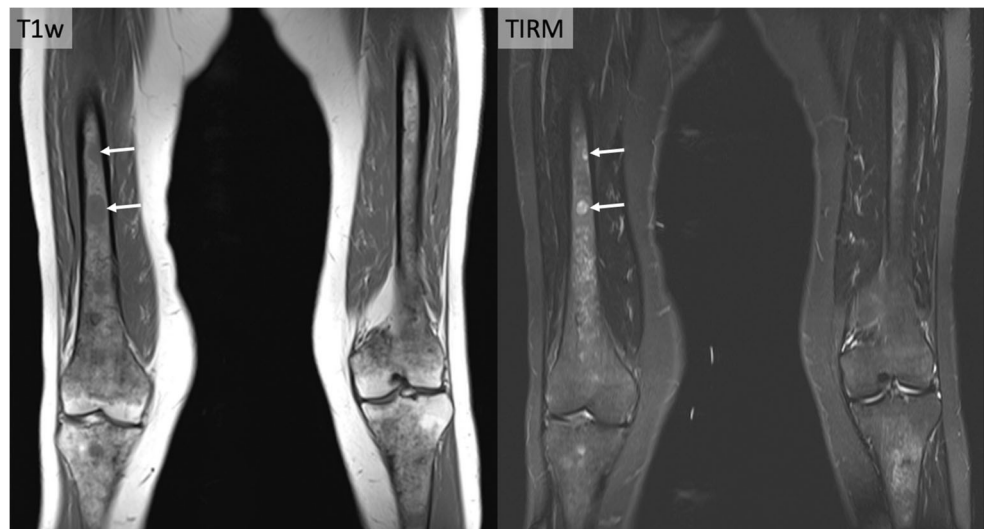
Fig. 5 Three patients with vertebral fractures in the lumbar spine. Classical multi-segmental osteoporotic fractures in a patient with indolent systemic mastocytosis (ISM)(a) and vertebral fractures in patients with advanced SM (AdvSM) with activated (b) and diffuse sclerotic (c) bone marrow, respectively



While fractures and osteolytic lesions are not appropriate to predict the severity of the disease, we found two distinct bone marrow patterns in patients with AdvSM, which are associated with a more aggressive form of the disease as activated and diffuse sclerotic BM are clearly correlated with a high MC burden (BM MC infiltration, serum tryptase, *KIT* D816V allele burden), organ damage (C-findings), and inferior survival.

In conclusion, pathologic (activated/sclerotic/small-spotted) BM changes of the spine and affection of the appendicular skeleton in patients with SM are indicative for the diagnosis of SSM or AdvSM. Particularly activated/sclerotic BM is associated with a high MC burden, organ damage, and adverse survival. Osteolytic lesions are overall very rare. Pathologic vertebral fractures are common in indolent and AdvSM; however, they resemble classical multi-segmental osteoporotic fractures only in ISM but not in AdvSM.

Fig. 6 72-year-old male patient with advanced systemic mastocytosis (AdvSM) showing focal osteolytic lesion of the femur (arrows)



Acknowledgments Karl Sotlar and Hans-Peter Horny are acknowledged for histological diagnosis.

Funding information This study was funded by the “Deutsche José Carreras Leukämie-Stiftung” (DJCLS 01 R/2018) and the SEED program of the Mannheim Medical Faculty, Heidelberg University, Heidelberg, Germany.

Compliance with ethical standards

Conflict of interest The authors declare no conflict of interest

Ethical approval All procedures performed in studies involving human participants were in accordance with the ethical standards of the institutional and/or national research committee and with the 1964 Helsinki declaration and its later amendments or comparable ethical standards.

Informed consent Informed consent was obtained from all individual participants included in the study.

References

1. Metcalfe DD (2008) Mast cells and mastocytosis. *Blood* 112:946–956
2. Valent P, Akin C, Sperr WR, Horny HP, Arock M, Lechner K, Bennett JM, Metcalfe DD (2003) Diagnosis and treatment of systemic mastocytosis: state of the art. *Br J Haematol* 122:695–717
3. Horny HP, Parwaresch MR, Lennert K (1985) Bone marrow findings in systemic mastocytosis. *Hum Pathol* 16:808–814
4. Arber DA, Orazi A, Hasserjian R et al (2016) The 2016 revision to the World Health Organization classification of myeloid neoplasms and acute leukemia. *Blood* 127:2391–2405
5. Valent P, Akin C, Metcalfe DD (2017) Mastocytosis: 2016 updated WHO classification and novel emerging treatment concepts. *Blood* 129:1420–1427
6. Tefferi A, Shah S, Reichard KK, Hanson CA, Pardanani A (2018) Smouldering mastocytosis: survival comparisons with indolent and aggressive mastocytosis. *Am J Hematol*. <https://doi.org/10.1002/ajh.25302>
7. Pardanani A (2016) Systemic mastocytosis in adults: 2017 update on diagnosis, risk stratification and management. *Am J Hematol* 91:1146–1159
8. Jawhar M, Schwaab J, Meggendorfer M, Naumann N, Horny HP, Sotlar K, Haferlach T, Schmitt K, Fabarius A, Valent P, Hofmann WK, Cross NCP, Metzgeroth G, Reiter A (2017) The clinical and molecular diversity of mast cell leukemia with or without associated hematologic neoplasm. *Haematologica* 102:1035–1043
9. Jawhar M, Schwaab J, Naumann N, Horny HP, Sotlar K, Haferlach T, Metzgeroth G, Fabarius A, Valent P, Hofmann WK, Cross NCP, Meggendorfer M, Reiter A (2017) Response and progression on midostaurin in advanced systemic mastocytosis: KIT D816V and other molecular markers. *Blood* 130:137–145
10. Jawhar M, Schwaab J, Schnittger S, Meggendorfer M, Pffirmann M, Sotlar K, Horny HP, Metzgeroth G, Kluger S, Naumann N, Haferlach C, Haferlach T, Valent P, Hofmann WK, Fabarius A, Cross NC, Reiter A (2016) Additional mutations in SRSF2, ASXL1 and/or RUNX1 identify a high-risk group of patients with KIT D816V(+) advanced systemic mastocytosis. *Leukemia* 30:136–143
11. Jawhar M, Schwaab J, Hausmann D, Clemens J, Naumann N, Henzler T, Horny HP, Sotlar K, Schoenberg SO, Cross NC, Fabarius A, Hofmann WK, Valent P, Metzgeroth G, Reiter A (2016) Splenomegaly, elevated alkaline phosphatase and mutations in the SRSF2/ASXL1/RUNX1 gene panel are strong adverse prognostic markers in patients with systemic mastocytosis. *Leukemia* 30:2342–2350
12. Schwaab J, Schnittger S, Sotlar K, Walz C, Fabarius A, Pffirmann M, Kohlmann A, Grossmann V, Meggendorfer M, Horny HP, Valent P, Jawhar M, Teichmann M, Metzgeroth G, Erben P, Ernst T, Hochhaus A, Haferlach T, Hofmann WK, Cross NC, Reiter A (2013) Comprehensive mutational profiling in advanced systemic mastocytosis. *Blood* 122:2460–2466
13. Metzgeroth G, Dinter D, Erben P, La Rosee P, Hehlmann R, Hastka J (2007) Systemic mastocytosis simulating osseous metastatic disease. *Br J Haematol* 136:1
14. Deb A, Tefferi A (2003) Images in clinical medicine. Systemic mastocytosis. *N Engl J Med* 349:e7
15. Myers B, Grimley C, Jones SG, Clark D, Kerslake R (2003) Skin, bone marrow and magnetic resonance imaging appearances in systemic mastocytosis. *Br J Haematol* 122:876
16. Epelboym Y, Keraliya AR, Tirumani SH, Hornick JL, Ramaiya NH, Shinagare AB (2017) Differences in the imaging features and distribution of non-indolent and indolent mastocytosis: a single institution experience of 29 patients. *Clin Imaging* 44:111–116
17. Huang TY, Yam LT, Li CY (1987) Radiological features of systemic mast-cell disease. *Br J Radiol* 60:765–770
18. Avila NA, Ling A, Metcalfe DD, Worobec AS (1998) Mastocytosis: magnetic resonance imaging patterns of marrow disease. *Skelet Radiol* 27:119–126
19. Roca M, Mota J, Giraldo P, Garcia Erce JA (1999) Systemic mastocytosis: MRI of bone marrow involvement. *Eur Radiol* 9:1094–1097
20. Siegel S, Sadler MA, Yook C, Chang V, Miller J (1999) Systemic mastocytosis with involvement of the pelvis: a radiographic and clinicopathologic study—a case report. *Clin Imaging* 23:245–248
21. Di Leo C, Lodi A, Pozzato C et al (2003) Systemic mastocytosis: bone marrow involvement assessed by Tc-99m MDP scintigraphy and magnetic resonance imaging. *Haematologica* 88:Ecr26
22. Sperr WR, Valent P (2012) Diagnosis, progression patterns and prognostication in mastocytosis. *Expert Rev Hematol* 5:261–274
23. Travis WD, Li CY, Bergstralh EJ, Yam LT, Swee RG (1988) Systemic mast cell disease. Analysis of 58 cases and literature review. *Medicine (Baltimore)* 67:345–368
24. Armingaud P, Zerkak D, Lespessailles E et al (2002) Bone evaluation in ten adults with cutaneous mastocytosis. *Ann Dermatol Venereol* 129:170–172
25. Grieser T, Minne HW (1997) Systemic mastocytosis and skeletal lesions. *Lancet* 350:1103–1104
26. Brunsen C, Hamdy NA, Papapoulos SE (2002) Osteoporosis and bone marrow mastocytosis: dissociation of skeletal responses and mast cell activity during long-term bisphosphonate therapy. *J Bone Miner Res* 17:567–569
27. Lim AY, Ostor AJ, Love S, Crisp AJ (2005) Systemic mastocytosis: a rare cause of osteoporosis and its response to bisphosphonate treatment. *Ann Rheum Dis* 64:965–966
28. Jawhar M, Schwaab J, Horny HP, Sotlar K, Naumann N, Fabarius A, Valent P, Cross NC, Hofmann WK, Metzgeroth G, Reiter A (2016) Impact of centralized evaluation of bone marrow histology in systemic mastocytosis. *Eur J Clin Investig* 46:392–397
29. Barete S, Assous N, de Gennes C, Grandpeix C, Feger F, Palmerini F, Dubreuil P, Arock M, Roux C, Launay JM, Fraïtag S, Canioni D, Billefont B, Suarez F, Lanternier F, Lortholary O, Hermine O, Francès C (2010) Systemic mastocytosis and bone involvement in a cohort of 75 patients. *Ann Rheum Dis* 69:1838–1841
30. Kluin-Nelemans HC, Jansen JH, Breukelman H et al (1992) Response to interferon alfa-2b in a patient with systemic mastocytosis. *N Engl J Med* 326:619–623

31. Rossini M, Zanotti R, Bonadonna P, Artuso A, Caruso B, Schena D, Vecchiato D, Bonifacio M, Viapiana O, Gatti D, Senna G, Riccio A, Passalacqua G, Pizzolo G, Adami S (2011) Bone mineral density, bone turnover markers and fractures in patients with indolent systemic mastocytosis. *Bone* 49:880–885
32. Manara M, Varenna M, Cantoni S, Parafioriti A, Gallazzi MB, Sinigaglia L (2010) Osteoporosis with vertebral fractures in young males, due to bone marrow mastocytosis: a report of two cases. *Clin Exp Rheumatol* 28:97–100
33. Theoharides TC, Boucher W, Spear K (2002) Serum interleukin-6 reflects disease severity and osteoporosis in mastocytosis patients. *Int Arch Allergy Immunol* 128:344–350
34. Brockow K, Akin C, Huber M, Metcalfe DD (2005) IL-6 levels predict disease variant and extent of organ involvement in patients with mastocytosis. *Clin Immunol* 115:216–223
35. Kanzaki S, Takahashi T, Kanno T, Ariyoshi W, Shinmyouzu K, Tujisawa T, Nishihara T (2008) Heparin inhibits BMP-2 osteogenic bioactivity by binding to both BMP-2 and BMP receptor. *J Cell Physiol* 216:844–850
36. Johansson C, Roupe G, Lindstedt G, Mellstrom D (1996) Bone density, bone markers and bone radiological features in mastocytosis. *Age Ageing* 25:1–7

Publisher's note Springer Nature remains neutral with regard to jurisdictional claims in published maps and institutional affiliations.